

Geophysical Research Letters[®]



RESEARCH LETTER

10.1029/2023GL106142

Recent Multi-Decadal Southern Ocean Surface Cooling Unlikely Caused by Southern Annular Mode Trends

Yue Dong^{1,2} , Lorenzo M. Polvani^{1,3} , and David B. Bonan⁴ 

¹Lamont-Doherty Earth Observatory, Columbia University, Palisades, NY, USA, ²Cooperative Programs for the Advancement of Earth System Science, University Corporation for Atmospheric Research, Boulder, CO, USA, ³Department of Applied Physics and Applied Mathematics, Columbia University, New York, NY, USA, ⁴Environmental Science and Engineering, California Institute of Technology, Pasadena, CA, USA

Key Points:

- Austral summer Southern Annular Mode (SAM) anomalies affect Southern Ocean (SO) sea-surface temperature (SST) only on seasonal to interannual timescales
- Multi-decadal observed SAM trends make little contribution to observed Southern Ocean SST trends
- Global climate models (GCMs) capture the observed seasonal SAM-SST relationship and yet fail to simulate the observed long-term SO cooling

Supporting Information:

Supporting Information may be found in the online version of this article.

Correspondence to:

Y. Dong,
dongyueatmos@gmail.com

Citation:

Dong, Y., Polvani, L. M., & Bonan, D. B. (2023). Recent multi-decadal Southern Ocean surface cooling unlikely caused by Southern Annular Mode trends. *Geophysical Research Letters*, 50, e2023GL106142. <https://doi.org/10.1029/2023GL106142>

Received 29 AUG 2023

Accepted 15 NOV 2023

Abstract Over recent decades, the Southern Ocean (SO) has experienced multi-decadal surface cooling despite global warming. Earlier studies have proposed that recent SO cooling has been caused by the strengthening of surface westerlies associated with a positive trend of the Southern Annular Mode (SAM) forced by ozone depletion. Here we revisit this hypothesis by examining the relationships between the SAM, zonal winds and SO sea-surface temperature (SST). Applying a low-frequency component analysis to observations, we show that while positive SAM anomalies can induce SST cooling as previously found, this seasonal-to-interannual modulation makes only a small contribution to the observed long-term SO cooling. Global climate models well capture the observed interannual SAM-SST relationship, and yet generally fail to simulate the observed multi-decadal SO cooling. The forced SAM trend in recent decades is thus unlikely the main cause of the observed SO cooling, pointing to a limited role of the Antarctic ozone hole.

Plain Language Summary Despite increasing greenhouse gases, the Southern Ocean sea-surface temperatures have cooled over the recent several decades. The cause of Southern Ocean cooling remains a puzzling feature of recent climate change. Earlier studies have proposed that this multi-decadal cooling in the Southern Ocean has arisen in part from the strengthening of surface winds associated with a positive trend in a mode of climate variability known as the Southern Annular Mode (SAM). Here we employ a new statistical method to examine this proposed relationship in both observations and climate models. We found that SAM variability only changes Southern Ocean surface temperature on short-term timescales and makes little contribution to observed long-term trends. Our results thus suggest the SAM trend, via the strengthening of circumpolar westerlies, is unlikely to be the main cause of the observed long-term Southern Ocean cooling.

1. Introduction

Unlike the Arctic, the Southern Ocean has experienced substantial cooling in recent decades, following an earlier warming period from the 1950s to 1980s (Figure 1a). This multi-decadal surface cooling over the Southern Ocean has been accompanied by anomalous surface freshening, sub-surface warming, and a slight positive trend in Antarctic sea-ice extent (Armour et al., 2016; De Lavergne et al., 2014; Fan et al., 2014; Parkinson, 2019; Roach et al., 2020), all of which remain puzzling features of the observed climate change in the Southern Hemisphere. Apart from its local impacts, Southern Ocean surface cooling has been found to have remote effects on the pattern of tropical surface warming (Dong, Armour, et al., 2022; Hwang et al., 2017; Kim et al., 2022), tropical atmospheric circulation (Kang et al., 2020, 2023), and estimates of the global warming rate and climate sensitivity (Dong, Pauling, et al., 2022).

Despite its broad impacts on both the local and global climate, the observed Southern Ocean SST trend remains poorly simulated by global climate models (GCMs) (Figure 1c). GCM initial-condition large ensembles (Deser et al., 2020a) generally produce too strong SO surface warming over recent decades (Wills et al., 2022), along with too weak surface freshening and positive trends in Antarctic sea-ice extent (Roach et al., 2020). These model deficiencies over the historical period thus call into question the reliability of model projections of future Antarctic climate change.

Several hypotheses have been put forward to explain the observed multi-decadal SO cooling, including SO natural variability driven by ocean convection (Cabr e et al., 2017; Latif et al., 2013; Polvani & Smith, 2013; Zhang et al., 2019), freshwater input from Antarctic ice-sheet melt (Bintanja et al., 2013; Pauling et al., 2016; Purich &

  2023 The Authors.

This is an open access article under the terms of the [Creative Commons Attribution-NonCommercial License](https://creativecommons.org/licenses/by-nc/4.0/), which permits use, distribution and reproduction in any medium, provided the original work is properly cited and is not used for commercial purposes.

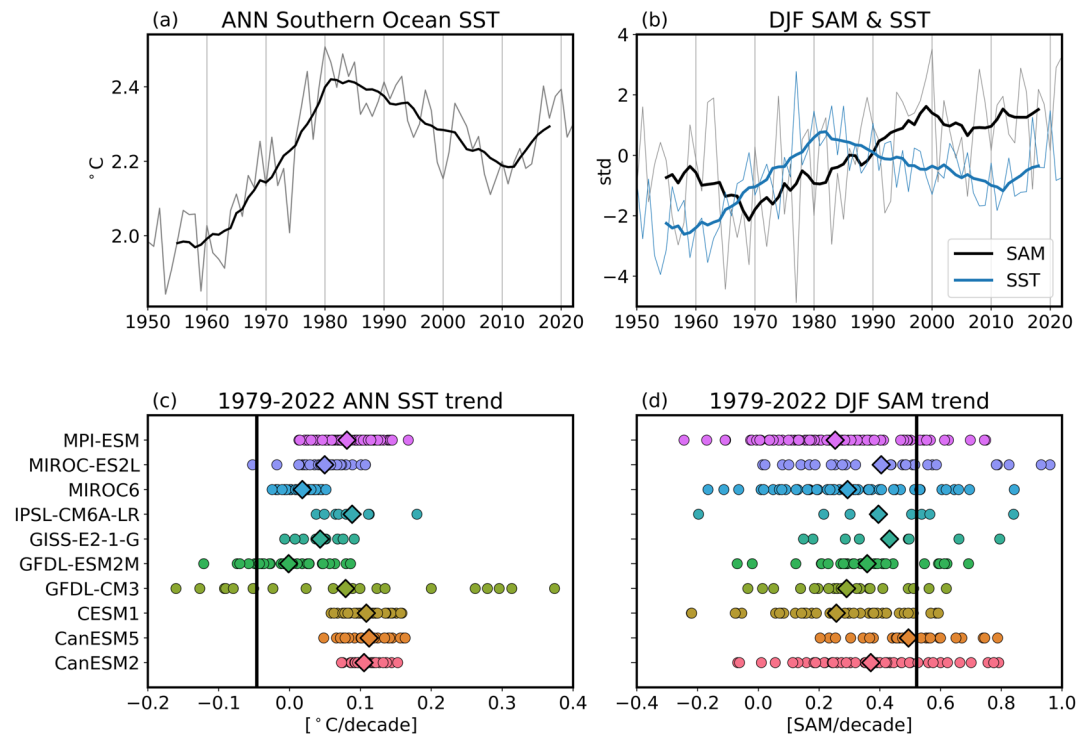


Figure 1. Observed and modeled Southern Ocean SST and SAM. (a) Observed annual-mean Southern Ocean SST (unit: $^{\circ}\text{C}$). (b) Normalized DJF SAM index and DJF SO SST index from observations (unit: standard deviation). In (a, b), thin lines denote annual data and thick lines denote 10-year running means. (c, d) Southern Ocean SST trend and the SAM trend over 1979–2022 in observations (black line) and model large-ensembles. Circles denote each individual ensemble member; diamonds denote ensemble mean.

England, 2023; Purich et al., 2018; Rye et al., 2020) or from northward sea-ice transport (Haumann et al., 2020). These hypotheses, however, are mostly built on modeling evidence, and are thus potentially subject to model biases. An alternative hypothesis is that the observed SO cooling trends may be driven by trends in surface westerlies via the Southern Annular Mode (SAM) through northward Ekman transport (Ferreira et al., 2015; Gupta & England, 2006; Hall & Visbeck, 2002; Lefebvre et al., 2004). It has been robustly observed that the surface westerlies have strengthened and shifted poleward, associated with the positive trend in the austral-summer (DJF) SAM over the second half of the 20th century (G. J. Marshall, 2003; Thompson & Solomon, 2002) (also Figure 1b). This trend in SAM has been in large part attributed to stratospheric ozone depletion (Banerjee et al., 2020; Polvani et al., 2011; Previdi & Polvani, 2014). The observed SAM trend is generally well captured in GCM simulations (Figure 1d) (Waugh et al., 2020).

To link SST variability to SAM variability, Doddridge and Marshall (2017) carried out an observational study and reported a robust interannual relationship between the SAM and SO SST. Their results show that positive SAM anomalies in the austral summer lead to anomalous cold SST persisting to the following autumn, suggesting a possible contribution of ozone depletion to SO cooling. On the modeling side, the SAM-SST connection on multi-decadal time scales was supported by idealized model simulations with abrupt SAM or ozone forcing (e.g., Ferreira et al., 2015; Kostov et al., 2018; Seviour et al., 2016). Early “step-like” forcing experiments showed a two-time-scale feature of the SO SST response to wind/SAM anomalies—a fast time-scale SST cooling response driven by the northward Ekman transport of surface waters and a slow time-scale SST warming response driven by the upwelling of warmer waters from below. Although a comprehensive study of such idealized experiments showed a very weak relationship between SAM and SST cooling on decadal time scales (Seviour et al., 2019), the appeal of a simple physical mechanism, the observed interannual modulation of SO SST by the SAM—and thus the Antarctic ozone hole—remains popular as a potential explanation of the multi-decadal cooling trends in the SO (Hartmann, 2022).

On the other hand, the causal relationship between SO SST trends and SAM or wind trends is at odds with several studies which have suggested that stratospheric ozone depletion causes surface *warming*, not cooling,

on multi-decadal time scale. Unlike the idealized abrupt-forcing simulations that show a “fast” SO cooling response, GCM simulations with realistic transient or time-averaged ozone forcing robustly simulate a SO warming response along with Antarctic sea-ice melting (Bitz & Polvani, 2012; Landrum et al., 2017; Sigmond & Fyfe, 2014; Smith et al., 2012). Additionally, a recent study by Polvani et al. (2021) re-examined the relationship between the SAM and Antarctic sea-ice extent (SIE) in observations and GCMs. They found that the interannual SAM modulation of Antarctic SIE only explains a small fraction of the year-to-year SIE variability, and thus does not account for multi-decadal SIE trends. These studies collectively suggest that SAM variability, associated with the ozone hole, is unlikely to be the main driver of the observed long-term trends in SO SST and Antarctic SIE, contradicting the conclusion of the idealized modeling studies.

Motivated by these discrepancies in previous findings, we aim to address two questions in this study: (a) Can GCMs simulate the observed interannual relationship between the SAM and SO SST? (b) To what extent does the interannual SAM modulation of SO SST contribute to the multi-decadal cooling trends in observations?

2. Interannual SAM Modulation of Southern Ocean SST

In this section, we first repeat the linear regression analysis in Doddridge and Marshall (2017) (hereafter “DM2017”) and Polvani et al. (2021) to re-examine the interannual SAM-SST relationship in both observations and GCMs. By comparing the results between observations and models, we assess whether model biases in long-term SO SST trends stem in part from model biases in the short-term SAM-SST modulation.

2.1. Data

For observations, we use SST from the NOAA Extended Reconstruction Sea Surface Temperature version 5 (ERSSTv5) data set (Huang et al., 2017a) and sea-level pressure (SLP) from the ERA5 Reanalysis data set (Hersbach et al., 2020a), both over the period of 1950–2022. For models, we use SST and SLP from 10 CMIP5 and CMIP6 models, including 5 models that participated in the multi-model large-ensemble project (Deser et al., 2020a) and 5 CMIP6 models that have large ensembles (>10 members) of historical and SSP simulations. The main difference between the CMIP5 and CMIP6 ensembles is that the historical simulations extend to 2005 for CMIP5 but to 2014 for CMIP6. Thus, for the period up until 2022, we use RCP8.5 scenario for CMIP5 models and SSP245 or SSP370 scenario for CMIP6 models (see Table S1 in Supporting Information S1). Because forcing scenarios share similar trajectories early on in the 21st century, we expect this to cause little variation across model ensembles (Lehner et al., 2020).

We compute the SO SST index as the spatial average of the SST over 50°S–70°S following DM2017. The DJF seasonal-mean SAM index is computed as the difference between zonal-mean SLP at 45°S and 60°S, normalized by the 1971–2000 average, following G. J. Marshall (2003). We focus on DJF SAM because the recent SAM trend is only significant in DJF (Swart & Fyfe, 2012; Waugh et al., 2020) and has been robustly attributed to stratospheric ozone depletion (Banerjee et al., 2020; Polvani et al., 2011). The same normalization is also applied to the DJF SST index to be compared with the DJF SAM index (Figure 1b). For both observations and GCM outputs, we remove the linear trend in DJF SAM and monthly SO SST timeseries over the entire period 1950–2022, before we perform the regression analysis.

2.2. Results

We begin with SO SST regressions against DJF SAM in observations, to examine whether DJF SAM anomalies are followed by anomalous SO SST. That is, we regress the timeseries of the DJF SAM index onto SO SST in every calendar month, ranging from the same year's December to next year's November. Figure 2 clearly shows that positive DJF SAM anomalies lead to SO SST cooling, which peaks in the same season (DJF) and gradually weakens in the following two seasons before eventually vanishing at the end of the year. This independently confirms the findings of DM2017, who showed that the SAM impact on SO SST (derived from a shorter time period of 1981–2017 in that study) is highly seasonal and does not persist over a year. Furthermore, our analysis reveals that the annually-averaged SST anomaly following a unit of positive SAM is only -0.05 K (Figure 2a) and the portion of SST variance explained (r^2) is merely 0.2 (Figure 2b). Therefore, while positive SAM can indeed lead to SO SST cooling, we emphasize that this modulation occurs only on a seasonal timescale and can barely

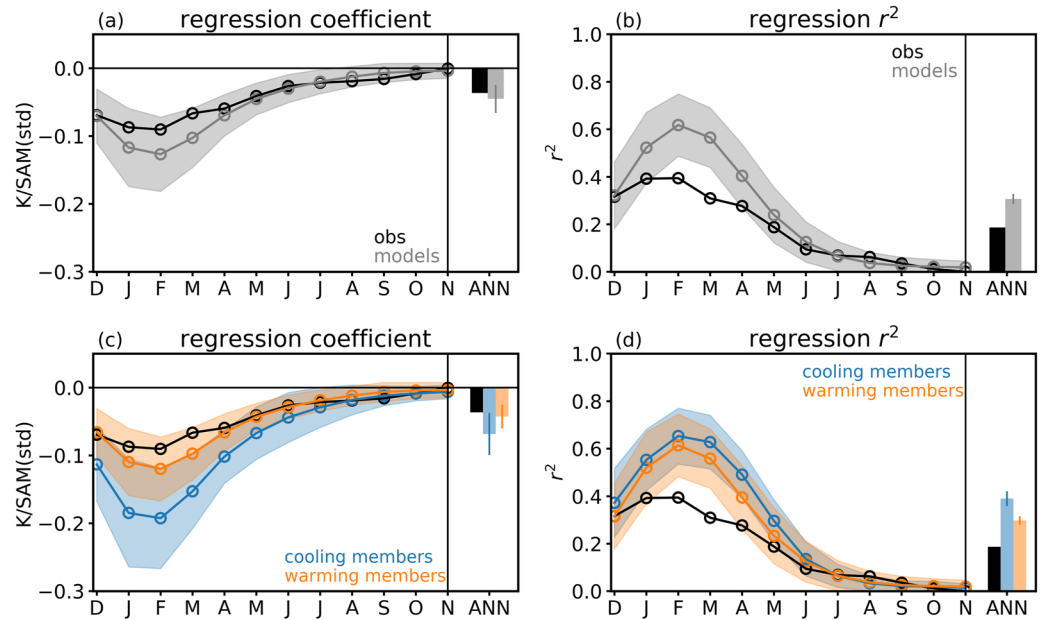


Figure 2. Regressions of monthly Southern Ocean SST (starting from DJF) onto same year's DJF SAM. (a–c) regression coefficient; (b–d) r^2 values of the regressions. Observations are shown in black, multi-model multi-ensemble means in gray, the ensemble members that simulate a negative SO SST trend over 1979–2022 (“cooling members”) in blue, and the members that simulate a positive SO SST trend (“warming members”) in orange. All shadings denote one standard deviation across ensemble members.

sustain at interannual or longer timescales. A similar result was reported by Polvani et al. (2021) for the DJF SAM modulation of Antarctic SIE.

Next, we repeat this regression analysis with model large ensembles. Perhaps surprisingly, models well reproduce the observed relationship between the DJF SAM and monthly SO SST (Figures 2a and 2b gray lines), despite failing to simulate multi-decadal SO cooling (Figure 1c). In fact, the multi-model mean regression even overestimates the maximum DJF SO SST cooling response and accounts for a higher SO SST variance (higher r^2) (also see Figures S1 and S2 in Supporting Information S1 for individual models).

To further investigate how the SAM modulation of SO SST impacts model-simulated long-term SST trends, we separate all model ensemble members (365 in total) into two groups: one consisting of all the members that simulate a negative trend of SO SST over 1979–2022 (35 members, blue lines in Figure 2) and the other consisting of the rest of members (330 members, orange lines in Figure 2). Although the ensemble members that can simulate the long-term SO cooling all produce a stronger SST cooling response to SAM, the members that fail to simulate the long-term cooling are also able to capture or even overestimate the observed SST response to SAM. These results suggest that correctly simulating the seasonal-to-interannual SAM modulation of SO SST does not guarantee the model's performance on multi-decadal SO SST trends, implying that short-term and long-term SST variability may be caused by different processes in models.

3. Low-Frequency Variability in the Southern Ocean

In the previous section, we have shown that in both observations and models the SO SST cooling response to positive SAM anomalies only occurs in the same and following seasons. This raises a key question: Given the observed long-term SAM trend, to what extent does the short-term SAM-SST relationship contribute to the observed long-term SO cooling?

In the case of Antarctic SIE, Polvani et al. (2021) addressed this question by comparing the actual SIE trend in observation with the estimate extrapolated from the linear SAM-SIE regression. They found that the SAM-regressed SIE trend is much smaller than the actual SIE trend even over the ozone depletion period (1980–2000) when the DJF SAM trend is most significant. They thus concluded that the SAM is not the major driver of the observed

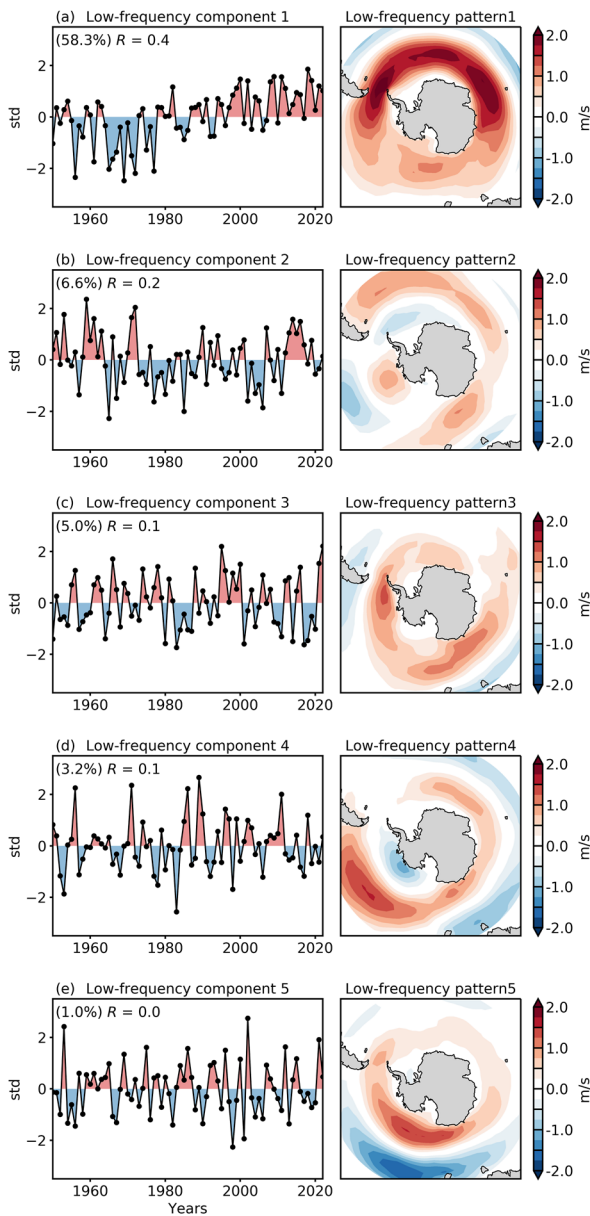


Figure 3. Low-frequency patterns (LFP; right column; unit: m/s) and their associated components (LFC; left column; unit: standard deviation) for the observed DJF U850 wind anomalies. Values in parentheses in the LFC panels denote the low-frequency variance explained by each mode. R values denote the ratio of low-frequency variance explained to the total variance, representing the signal-to-noise ratio.

long-term SIE trend. We performed the same linear analysis for the SO SST and found a similar result: the annual-mean SO SST trend inferred from the SAM trend during 1979–2022 accounts for only 40% of the actual SO SST trend, although the contribution increases to 70% for the SST trend in DJF. However, several caveats must be noted in such simple trend attribution. First, the results are sensitive to the period over which the trend is calculated, as SAM and SO SST appear to vary *non-synchronously* (Figure 1b). For example, during the period of maximum SAM trend (1970s to 2000s), the strong SAM trend and the linear relationship would have suggested a SO cooling trend ($-0.09^{\circ}\text{C}/\text{decade}$ in DJF) that is unrealistically stronger than the actual observed SST trend ($0^{\circ}\text{C}/\text{decade}$). Whereas during the period of maximum SO cooling (1980s to 2010s), the SAM trend only explained 23% of the actual annual-mean SST trend and 45% in DJF. Second, such an analysis using the zonal-mean SAM index overlooks the spatial heterogeneity in the variability of wind and SST, and therefore provides no information on the spatial contribution of wind to observed SST trend patterns. Thus, in this section, we revisit this question by employing a novel statistical method called low-frequency component analysis (LFCA; Wills et al., 2018), to identify modes of low-frequency variability in observed zonal winds and the SST changes associated with them.

3.1. LFCA Method

LFCA (Wills et al., 2018) is a relatively new statistical technique—similar to the conventional principal component analysis—to compute a linear combination of empirical orthogonal functions (EOFs). LFCA maximizes the ratio of low-pass filtered variance to total variance, such that it isolates leading modes of low-frequency variability and extracts physically-based modes in spatial-temporal signals in climate fields. It has been applied to examine a wide range of climate quantities, including variability in global SST anomalies (Wills et al., 2022), Atlantic ocean heat transport (Oldenburg et al., 2021), and Arctic and Antarctic sea-ice concentration (Bonan et al., 2023; Dörr et al., 2023).

There are several advantages of using LFCA to investigate the relationship between long-term SAM and SST. First, it helps separate low-frequency (decadal to multi-decadal) and high-frequency (interannual) variability in SAM, allowing us to isolate the long-term contribution of SAM to SST trends. Second, instead of directly using the simpler zonal-mean SAM time-series, we apply LFCA to the observed zonal winds at 850 hPa at each latitude and longitude and find the timeseries associated with the leading mode of wind variability. This gives us a more complete understanding of the relationship between winds and SST as it accounts for spatial variability of winds and SST. This is important because several recent studies have pointed out the non-zonal feature of the observed SAM-associated wind changes (Vaugh et al., 2020) and its zonally asymmetric impacts on SO and remote SSTs (Dong, Armour, et al., 2022).

Our analysis uses the zonal winds at 850 hPa (U850) from the ERA5 Reanalysis data set (Hersbach et al., 2020a). We use the raw data, without removing the linear trends, in order to account for all temporal variability. As with the SAM index analyzed in Section 2, we consider DJF U850 over 1950–2022. We apply LFCA to the reanalysis U850 only over 40°S – 80°S , to avoid variability associated with tropical winds. Our LFCA uses a 15-year cutoff low-pass filter to isolate low-frequency variability, and we retain the 5 leading EOFs, which account for 77% of the total U850 variability (we find that increasing the number of EOFs does not lead to substantially more variance explained). The LFCA results remain the same regardless of whether we choose a low-pass filter of 10 years, 15 years or 20 years (compare Figure S3 in Supporting Information S1 to Figure 3).

3.2. LFCA Results

First, let us consider the leading anomaly patterns (i.e., low-frequency patterns, LFPs) and their associated time-series (i.e., low-frequency components, LFCs) obtained by applying LFCA to the reanalysis DJF U850 over the Southern Ocean. The first 5 LFPs and LFCs are shown in Figure 3, in the left and right columns, respectively.

The leading mode (LFP1) features a SAM-like annular pattern of wind strengthening that has increased monotonically from 1970s to 2000s (see LFC1). This is well in line with the SAM trend caused by ozone depletion (Banerjee et al., 2020). This mode accounts for 58.3% of the low-frequency variance and has the highest signal-to-noise ratio of 0.4. The next four modes exhibit mostly non-zonal patterns (LFP2–5), where wind anomalies are confined to specific ocean sectors. The LFCs associated with LFP2 and LFP3 have some decadal-to-multi-decadal variability, while the LFCs associated with LFP4 and LFP5 are dominated by interannual variability, consistent with their low signal-to-noise ratio.

Next, we examine the U850 trend pattern (1979–2022) associated with each mode by projecting each LFC onto the corresponding LFP of U850 at each grid point over the SO. Figure S4 in Supporting Information S1 confirms that the total reconstruction based on the five LFPs (Figure S4b in Supporting Information S1) well reproduces the observed U850 trend pattern (Figure S4a in Supporting Information S1), which is characterized by a strengthening of the westerlies at high latitudes in the Southern Ocean. Furthermore, the total reconstructed trend pattern remains the same using either the leading five or three LFPs, suggesting that LFP 1–3 are the major contributor to the total U850 trends over recent decades.

3.3. Long-Term Relationship Between SO SST and Winds

Having established that the leading modes obtained by LFCA well reproduce the observed U850 trend pattern, we next investigate the long-term relationship between U850 and SO SST by examining how each LFP and LFC influences SST across timescales.

First, we regress the observed DJF SST over the entire period (1950–2022) at each grid box onto the LFC time-series associated with the three leading wind LFPs, respectively (Figures 4a–4c). We focus on DJF as our earlier results suggest it is the season when the SAM, through surface winds, has the strongest impact on SST. Consistent with the SAM-SST regression result (Figure 2), the wind LFC-SST regression also shows broad SST cooling anomalies around Antarctica associated with positive LFC anomalies. However, it is interesting that the patterns of SST cooling response do not quite match the wind anomaly patterns (compare Figures 3 and 4): All three wind LFPs feature positive wind anomalies throughout the Southern Ocean (LFP1 even has stronger wind anomalies in the Atlantic basin than in the Pacific basin), yet their SST cooling responses are most significant in the Pacific basin. This mismatch in spatial patterns indicates that there may be several mechanisms responsible for the SST response to wind, beyond zonal-mean Ekman heat transport.

Second, we estimate the long-term SST trends over the period 1979–2022 based on the above linear regression. Specifically, we multiply the regression between each LFC and SST at each grid box with the corresponding LFP, and then take the linear trend of the reconstructed SST timeseries at each grid box (Figure 4). Although the LFC-based SST trends also occur in the Pacific basin—consistent with observations—one immediately sees that the magnitudes of wind-driven SST trends are much weaker than that observed (cf. Figure 4 middle row vs. Figure 4g). Taking a spatial average over the Pacific sector of the Southern Ocean where the observed SST cooling is strongest (150°E–60°W, 50°S–70°S), we obtain an SST trend of $-0.098^{\circ}\text{C}/\text{decade}$ from the observation, and SST trends of -0.025 , -0.014 , and $-0.002^{\circ}\text{C}/\text{decade}$ from LFC1–3 regressions respectively, which altogether account for less than half of the actual SST trend (Figure 4i). To further illustrate the inability of winds to account for the time-evolution of SO SST, we plot the timeseries of DJF SO SST anomalies (relative to their climatology) for the observation and for the estimates using LFC1–3 regressions (Figure 4h). Although each of the LFCs contributes to some SST variability, none of them can produce a multi-decadal SO SST variability as strong as the observed timeseries. Even the sum of all three LFC-regression-based SO SST timeseries fails to explain the much larger multi-decadal trends in the observed SO SST.

Furthermore, our SST trend estimates so far have been focused on DJF, in the same season with wind anomalies, so as to capture the strongest wind impacts on SST. We also repeated the analysis for annual-mean (instead of DJF only) SST (Figure S5 in Supporting Information S1). The annual-mean SST anomalies following a unit of DJF wind LFC changes are even weaker, leading to almost negligible wind-driven annual-mean SST trends over

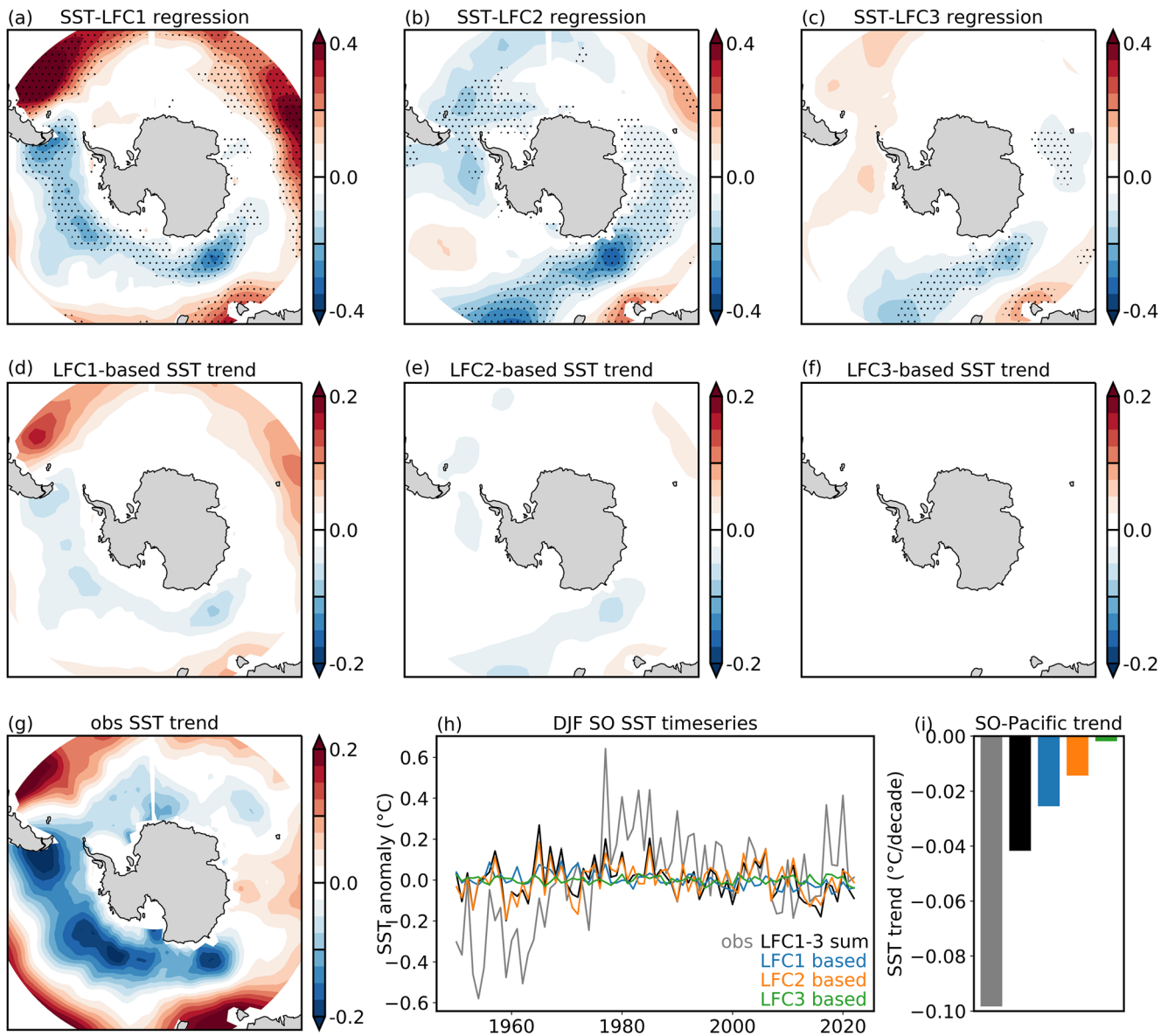


Figure 4. (a–c) DJF SST regression map onto LFC1–3 respectively (unit: °C/std). Stippling indicates where linear regression is statistically significant at 95% level. (d–g) DJF SST trend patterns over 1979–2022 (°C/decade) estimated from regressions with LFC 1–3 respectively and ERSSTv5. (h) Timeseries of SO SST anomalies relative to their climatology and (i) SST trends averaged over the Pacific sector (150°E–60°W, 50°S–70°S, the region with the strongest SST cooling), from the observation (gray), the regressions with LFC1–3 respectively (colored), and all three leading LFCs (black).

recent decades, that is, $-0.016^{\circ}\text{C}/\text{decade}$ over 1979–2022 from all three leading-mode regressions, compared to $-0.09^{\circ}\text{C}/\text{decade}$ of the actual SST trend (Figure S5j in Supporting Information S1).

Thus, by projecting SO SST onto the leading modes of observed wind variability, we find that although positive DJF wind anomalies can cause some SST cooling in the same season, this modulation does not survive more than a few months, and the resulting wind-driven SST cooling is too weak to explain the large multi-decadal trend in the observed Southern Ocean SST (Figure 4). Hence, the recent wind strengthening over the Southern Ocean is unlikely the key driver of the long-term Southern Ocean cooling.

4. Summary and Discussion

In this study, we have re-examined a previously proposed idea that positive SAM anomalies in DJF, associated with a strengthening of the circumpolar westerlies, may in part explain the observed Southern Ocean cooling

(Doddridge & Marshall, 2017; Ferreira et al., 2015; J. Marshall et al., 2014; Kostov et al., 2018). Using GCM large-ensembles, we have found that models are able to capture the observed seasonal-to-interannual modulation of SO SST by the SAM, regardless of whether they are able to simulate the long-term SO cooling. Focusing on observations, we have shown that although positive SAM anomalies and positive zonal wind anomalies in DJF can lead to some SST cooling anomalies in the same season, this mechanism only operates for a few months and does not persist from year to year. Computing SST trends from SAM trends alone, and noting the mismatch between SAM and SO SST trends, we conclude that the weak SST response to SAM on the fast timescale is unable to explain the observed multi-decadal Southern Ocean cooling.

One novel aspect of our study is that we used a low-frequency component analysis to isolate trends in SO zonal winds, rather than focusing on SAM trend alone. While the SAM index has been widely used as a metric to quantify zonal wind changes in the Southern Hemisphere, it only represents zonal-mean features and includes a wide range of variabilities from interannual to decadal timescales. Applying LFCA to the observed wind anomalies has allowed us to (a) obtain the timeseries (LFCs) of the leading modes of wind variability while retaining the spatial pattern of the wind anomalies, and (b) disentangle low-frequency from high-frequency variability.

It could be argued that the weak connection between long-term SAM and SST trends can be immediately deduced from the SAM and SST timeseries alone. Although Southern Ocean SST observations prior to the satellite era may bear large uncertainty due to insufficient data sampling, a simple visual inspection of their smoothed timeseries in recent decades (thick curves in Figure 1b) suffices to note that the kinks in those curves do not match. The SST cooling starts after 1980 and persists past 2010, whereas the positive SAM trend starts well before 1970 and stops after 2000, as a consequence of the Montreal Protocol (Banerjee et al., 2020). Building on this, our new analysis, accounting for spatial-temporal variability, adds additional evidence corroborating the inability of the SAM and surface westerlies to explain the recent multi-decadal SO cooling.

Understanding the causes of the observed Southern Ocean cooling and biases in climate models remains a major challenge. While we showed models well reproduce the observed fast SST response to SAM (Figure 2), another study (Purich et al., 2016) has found biases in model simulated SAM trends and argued for the linkage between underestimated wind trends and the lack of cooling in models, although that conclusion may be a consequence of not having separately estimated the pre- and post-ozone depletion trends. On the other hand, recent modeling work has shown that nudging tropospheric wind anomalies around Antarctica toward observations in a GCM (CESM1) does not reproduce the observed SO cooling over recent four decades (Blanchard-Wigglesworth et al., 2021; Dong, Armour, et al., 2022), providing evidence that model biases in SO SST trends are not simply a result of biases in simulated winds and SAM. Our study further adds observational evidence that the fast SST response to SAM makes little contribution to the observed long-term SST trend. These results collectively suggest a possibly limited role of stratospheric ozone depletion in driving the long-term SO SST trend.

Beyond potential remote impacts from the tropics, other local contributors to the recent SO cooling remain plausible, including freshwater input from Antarctic ice-sheet melt (Bintanja et al., 2013; Dong, Pauling, et al., 2022; Purich et al., 2018; Rye et al., 2020) or northward sea-ice transport (Haumann et al., 2020), and Southern Ocean natural variability (Cabr e et al., 2017; Latif et al., 2013; Zhang et al., 2019). Whether the recent SO cooling was driven by historical forcings or simply reflects natural variability has important implications for SST trends in the near future. Accurately constraining future projections of Antarctic climate change thus requires a better understanding of the causes of the recent multi-decadal Southern Ocean SST trends.

Data Availability Statement

We use SST from the ERSSTv5 data set (Huang et al., 2017a, 2017b), and atmospheric reanalysis from ERA5 Reanalysis (Hersbach et al., 2020a, 2020b). CMIP5 and CMIP6 multi-model large ensembles (Deser et al., 2020a) are available via the NCAR Climate Data Gateway (Deser et al., 2020b) and the ESGF CMIP data archive (Cinquini et al., 2014).

Acknowledgments

We thank Edward Doddridge and another anonymous reviewer for constructive comments. YD was supported by the NOAA Climate and Global Change Postdoctoral Fellowship Program, administered by UCAR's Cooperative Programs for the Advancement of Earth System Science (CPAESS) under award NA210AR4310383. DBB was supported by the National Science Foundation (NSF) Graduate Research Fellowship Program (NSF Grant DGE-1745301). LMP is grateful to the US NSF for their continued support, under award #1914569.

References

Armour, K. C., Marshall, J., Scott, J. R., Donohoe, A., & Newsom, E. R. (2016). Southern Ocean warming delayed by circumpolar upwelling and equatorward transport. *Nature Geoscience*, 9(7), 549–554. <https://doi.org/10.1038/ngeo2731>

Banerjee, A., Fyfe, J. C., Polvani, L. M., Waugh, D., & Chang, K.-L. (2020). A pause in Southern Hemisphere circulation trends due to the Montreal Protocol. *Nature*, 579(7800), 544–548. <https://doi.org/10.1038/s41586-020-2120-4>

Bintanja, R., van Oldenborgh, G. J., Drijfhout, S., Wouters, B., & Katsman, C. (2013). Important role for ocean warming and increased ice-shelf melt in Antarctic sea-ice expansion. *Nature Geoscience*, 6(5), 376–379. <https://doi.org/10.1038/ngeo1767>

Bitz, C., & Polvani, L. M. (2012). Antarctic climate response to stratospheric ozone depletion in a fine resolution ocean climate model. *Geophysical Research Letters*, 39(20), L20705. <https://doi.org/10.1029/2012gl053393>

Blanchard-Wrigglesworth, E., Roach, L. A., Donohoe, A., & Ding, Q. (2021). Impact of winds and Southern Ocean SSTs on Antarctic sea ice trends and variability. *Journal of Climate*, 34(3), 949–965. <https://doi.org/10.1175/jcli-d-20-0386.1>

Bonan, D. B., Dörr, J., Wills, R. C., Thompson, A. F., & Årthun, M. (2023). Sources of low-frequency variability in observed Antarctic sea ice. *EGU sphere*, 1–28.

Cabr e, A., Marinov, I., & Gnanadesikan, A. (2017). Global atmospheric teleconnections and multidecadal climate oscillations driven by Southern Ocean convection. *Journal of Climate*, 30(20), 8107–8126. <https://doi.org/10.1175/jcli-d-16-0741.1>

Cinquin, L., Crichton, D., Mattmann, C., Harney, J., Shipman, G., Wang, F., et al. (2014). The Earth System Grid Federation: An open infrastructure for access to distributed geospatial data [Dataset]. *Future Generation Computer Systems*, 36, 400–417. <https://doi.org/10.1016/j.future.2013.07.002>

De Lavergne, C., Palter, J. B., Galbraith, E. D., Bernardello, R., & Marinov, I. (2014). Cessation of deep convection in the open Southern Ocean under anthropogenic climate change. *Nature Climate Change*, 4(4), 278–282. <https://doi.org/10.1038/nclimate2132>

Deser, C., Lehner, F., Rodgers, K. B., Ault, T., Delworth, T. L., DiNezio, P. N., et al. (2020a). Insights from Earth system model initial-condition large ensembles and future prospects. *Nature Climate Change*, 10(4), 277–286. <https://doi.org/10.1038/s41558-020-0731-2>

Deser, C., Lehner, F., Rodgers, K. B., Ault, T., Delworth, T. L., DiNezio, P. N., et al. (2020b). Multi-model large ensemble archive (MMELA) [Dataset]. Climate Data Gateway at NCAR. https://www.earthsystemgrid.org/dataset/ucar.cgd.cesm4.CLIVAR_LE.html/

Doddridge, E. W., & Marshall, J. (2017). Modulation of the seasonal cycle of Antarctic sea ice extent related to the Southern Annular Mode. *Geophysical Research Letters*, 44(19), 9761–9768. <https://doi.org/10.1002/2017gl074319>

Dong, Y., Armour, K. C., Battisti, D. S., & Blanchard-Wrigglesworth, E. (2022). Two-way teleconnections between the Southern Ocean and the tropical Pacific via a dynamic feedback. *Journal of Climate*, 35(19), 1–37. <https://doi.org/10.1175/jcli-d-22-0080.1>

Dong, Y., Pauling, A. G., Sadai, S., & Armour, K. C. (2022). Antarctic ice-sheet meltwater reduces transient warming and climate sensitivity through the sea-surface temperature pattern effect. *Geophysical Research Letters*, 49(24), e2022GL101249. <https://doi.org/10.1029/2022gl101249>

Dörr, J. S., Bonan, D. B., Årthun, M., Svendsen, L., & Wills, R. C. (2023). Forced and internal components of observed Arctic sea-ice changes. *The Cryosphere Discussions*, 17(9), 1–27. <https://doi.org/10.5194/tc-17-4133-2023>

Fan, T., Deser, C., & Schneider, D. P. (2014). Recent Antarctic sea ice trends in the context of Southern Ocean surface climate variations since 1950. *Geophysical Research Letters*, 41(7), 2419–2426. <https://doi.org/10.1002/2014gl059239>

Ferreira, D., Marshall, J., Bitz, C. M., Solomon, S., & Plumb, A. (2015). Antarctic Ocean and sea ice response to ozone depletion: A two-time-scale problem. *Journal of Climate*, 28(3), 1206–1226. <https://doi.org/10.1175/jcli-d-14-00313.1>

Gupta, A. S., & England, M. H. (2006). Coupled ocean–atmosphere–ice response to variations in the southern annular mode. *Journal of Climate*, 19(18), 4457–4486. <https://doi.org/10.1175/jcli3843.1>

Hall, A., & Visbeck, M. (2002). Synchronous variability in the Southern Hemisphere atmosphere, sea ice, and ocean resulting from the annular mode. *Journal of Climate*, 15(21), 3043–3057. [https://doi.org/10.1175/1520-0442\(2002\)015<3043:svtish>2.0.co;2](https://doi.org/10.1175/1520-0442(2002)015<3043:svtish>2.0.co;2)

Hartmann, D. L. (2022). The Antarctic ozone hole and the pattern effect on climate sensitivity. *Proceedings of the National Academy of Sciences of the United States of America*, 119(35), e2207889119. <https://doi.org/10.1073/pnas.2207889119>

Haumann, F. A., Gruber, N., & Münnich, M. (2020). Sea-ice induced southern ocean subsurface warming and surface cooling in a warming climate. *AGU Advances*, 1(2), e2019AV000132. <https://doi.org/10.1029/2019av000132>

Hersbach, H., Bell, B., Berrisford, P., Hirahara, S., Horányi, A., Muñoz-Sabater, J., et al. (2020a). The ERA5 global reanalysis. *Quarterly Journal of the Royal Meteorological Society*, 146(730), 1999–2049. <https://rmetes.onlinelibrary.wiley.com/doi/10.1002/qj.3803>

Hersbach, H., Bell, B., Berrisford, P., Hirahara, S., Horányi, A., Muñoz-Sabater, J., et al. (2020b). ERA5 monthly averaged data on pressure levels from 1940 to present [Dataset]. Copernicus Climate Service. <https://cds.climate.copernicus.eu/cdsapp#!/dataset/reanalysis-era5-pressure-levels-monthly-mean>

Huang, B., Thorne, P. W., Banzon, V. F., Boyer, T., Chepurin, G., Lawrimore, J. H., et al. (2017a). Extended reconstructed sea surface temperature, version 5 (ERSSTv5): Upgrades, validations, and intercomparisons. *Journal of Climate*, 30(20), 8179–8205. <https://doi.org/10.1175/jcli-d-16-0836.1>

Huang, B., Thorne, P. W., Banzon, V. F., Boyer, T., Chepurin, G., Lawrimore, J. H., et al. (2017b). NOAA extended reconstructed sea surface temperature (ERSST), version 5 [Dataset]. NOAA National Centers for Environmental Information. <https://downloads.psl.noaa.gov/Datasets/noaa.ersst.v5/>

Hwang, Y.-T., Xie, S.-P., Deser, C., & Kang, S. M. (2017). Connecting tropical climate change with southern ocean heat uptake. *Geophysical Research Letters*, 44(18), 9449–9457. <https://doi.org/10.1002/2017gl074972>

Kang, S. M., Xie, S.-P., Shin, Y., Kim, H., Hwang, Y.-T., Stuecker, M. F., et al. (2020). Walker circulation response to extratropical radiative forcing. *Science Advances*, 6(47), eabd3021. <https://doi.org/10.1126/sciadv.abd3021>

Kang, S. M., Yu, Y., Deser, C., Zhang, X., Kang, I.-S., Lee, S.-S., et al. (2023). Global impacts of recent Southern Ocean cooling. *Proceedings of the National Academy of Sciences of the United States of America*, 120(30), e2300881120. <https://doi.org/10.1073/pnas.2300881120>

Kim, H., Kang, S. M., Kay, J. E., & Xie, S.-P. (2022). Subtropical clouds key to Southern Ocean teleconnections to the tropical Pacific. *Proceedings of the National Academy of Sciences of the United States of America*, 119(34), e2200514119. <https://doi.org/10.1073/pnas.2200514119>

Kostov, Y., Ferreira, D., Armour, K. C., & Marshall, J. (2018). Contributions of greenhouse gas forcing and the Southern Annular Mode to historical Southern Ocean surface temperature trends. *Geophysical Research Letters*, 45(2), 1086–1097. <https://doi.org/10.1002/2017gl074964>

Landrum, L. L., Holland, M. M., Raphael, M. N., & Polvani, L. M. (2017). Stratospheric ozone depletion: An unlikely driver of the regional trends in Antarctic sea ice in austral fall in the late twentieth century. *Geophysical Research Letters*, 44(21), 11–062. <https://doi.org/10.1002/2017gl075618>

Latif, M., Martin, T., & Park, W. (2013). Southern Ocean sector centennial climate variability and recent decadal trends. *Journal of Climate*, 26(19), 7767–7782. <https://doi.org/10.1175/jcli-d-12-00281.1>

- Lefebvre, W., Goosse, H., Timmermann, R., & Fichefet, T. (2004). Influence of the Southern Annular Mode on the sea ice–ocean system. *Journal of Geophysical Research*, 109(C9), C09005. <https://doi.org/10.1029/2004jc002403>
- Lehner, F., Deser, C., Maher, N., Marotzke, J., Fischer, E. M., Brunner, L., et al. (2020). Partitioning climate projection uncertainty with multiple large ensembles and CMIP5/6. *Earth System Dynamics*, 11(2), 491–508. <https://doi.org/10.5194/esd-11-491-2020>
- Marshall, G. J. (2003). Trends in the Southern Annular Mode from observations and reanalyses. *Journal of Climate*, 16(24), 4134–4143. [https://doi.org/10.1175/1520-0442\(2003\)016<4134:titsam>2.0.co;2](https://doi.org/10.1175/1520-0442(2003)016<4134:titsam>2.0.co;2)
- Marshall, J., Armour, K. C., Scott, J. R., Kostov, Y., Hausmann, U., Ferreira, D., et al. (2014). The ocean's role in polar climate change: Asymmetric Arctic and Antarctic responses to greenhouse gas and ozone forcing. *Philosophical Transactions of the Royal Society A: Mathematical, Physical & Engineering Sciences*, 372(2019), 20130040. <https://doi.org/10.1098/rsta.2013.0040>
- Oldenburg, D., Wills, R. C., Armour, K. C., Thompson, L., & Jackson, L. C. (2021). Mechanisms of low-frequency variability in North Atlantic Ocean heat transport and AMOC. *Journal of Climate*, 34(12), 4733–4755.
- Parkinson, C. L. (2019). A 40-y record reveals gradual Antarctic sea ice increases followed by decreases at rates far exceeding the rates seen in the Arctic. *Proceedings of the National Academy of Sciences of the United States of America*, 116(29), 14414–14423. <https://doi.org/10.1073/pnas.1906556116>
- Pauling, A. G., Bitz, C. M., Smith, I. J., & Langhorne, P. J. (2016). The response of the Southern Ocean and Antarctic sea ice to freshwater from ice shelves in an Earth system model. *Journal of Climate*, 29(5), 1655–1672. <https://doi.org/10.1175/jcli-d-15-0501.1>
- Polvani, L. M., Banerjee, A., Chemke, R., Doddridge, E., Ferreira, D., Gnanadesikan, A., et al. (2021). Interannual Sam modulation of Antarctic sea ice extent does not account for its long-term trends, pointing to a limited role for ozone depletion. *Geophysical Research Letters*, 48(21), e2021GL094871. <https://doi.org/10.1029/2021gl094871>
- Polvani, L. M., & Smith, K. L. (2013). Can natural variability explain observed Antarctic sea ice trends? New modeling evidence from CMIP5. *Geophysical Research Letters*, 40(12), 3195–3199. <https://doi.org/10.1002/grl.50578>
- Polvani, L. M., Waugh, D. W., Correa, G. J., & Son, S.-W. (2011). Stratospheric ozone depletion: The main driver of twentieth-century atmospheric circulation changes in the Southern Hemisphere. *Journal of Climate*, 24(3), 795–812. <https://doi.org/10.1175/2010jcli3772.1>
- Previdi, M., & Polvani, L. M. (2014). Climate system response to stratospheric ozone depletion and recovery. *Quarterly Journal of the Royal Meteorological Society*, 140(685), 2401–2419. <https://doi.org/10.1002/qj.2330>
- Purich, A., Cai, W., England, M. H., & Cowan, T. (2016). Evidence for link between modelled trends in Antarctic sea ice and underestimated westerly wind changes. *Nature Communications*, 7(1), 10409. <https://doi.org/10.1038/ncomms10409>
- Purich, A., & England, M. H. (2023). Projected impacts of Antarctic meltwater anomalies over the twenty-first century. *Journal of Climate*, 36(8), 2703–2719. <https://doi.org/10.1175/jcli-d-22-0457.1>
- Purich, A., England, M. H., Cai, W., Sullivan, A., & Durack, P. J. (2018). Impacts of broad-scale surface freshening of the Southern Ocean in a coupled climate model. *Journal of Climate*, 31(7), 2613–2632. <https://doi.org/10.1175/jcli-d-17-0092.1>
- Roach, L. A., Dörr, J., Holmes, C. R., Massonnet, F., Blockley, E. W., Notz, D., et al. (2020). Antarctic sea ice area in CMIP6. *Geophysical Research Letters*, 47(9), e2019GL086729. <https://doi.org/10.1029/2019gl086729>
- Rye, C. D., Marshall, J., Kelley, M., Russell, G., Nazarenko, L. S., Kostov, Y., et al. (2020). Antarctic glacial melt as a driver of recent Southern Ocean climate trends. *Geophysical Research Letters*, 47(11), e2019GL086892. <https://doi.org/10.1029/2019gl086892>
- Seviour, W. J. M., Codron, F., Doddridge, E. W., Ferreira, D., Gnanadesikan, A., Kelley, M., et al. (2019). The Southern Ocean sea surface temperature response to ozone depletion: A multimodel comparison. *Journal of Climate*, 32(16), 5107–5121. <https://doi.org/10.1175/jcli-d-19-0109.1>
- Seviour, W. J. M., Gnanadesikan, A., & Waugh, D. W. (2016). The transient response of the Southern Ocean to stratospheric ozone depletion. *Journal of Climate*, 29(20), 7383–7396. <https://doi.org/10.1175/jcli-d-16-0198.1>
- Sigmond, M., & Fyfe, J. C. (2014). The Antarctic sea ice response to the ozone hole in climate models. *Journal of Climate*, 27(3), 1336–1342. <https://doi.org/10.1175/jcli-d-13-00590.1>
- Smith, K. L., Polvani, L. M., & Marsh, D. R. (2012). Mitigation of 21st century Antarctic sea ice loss by stratospheric ozone recovery. *Geophysical Research Letters*, 39(20), L20701. <https://doi.org/10.1029/2012gl053325>
- Swart, N., & Fyfe, J. C. (2012). Observed and simulated changes in the Southern Hemisphere surface westerly wind-stress. *Geophysical Research Letters*, 39(16), L16711. <https://doi.org/10.1029/2012gl052810>
- Thompson, D. W., & Solomon, S. (2002). Interpretation of recent Southern Hemisphere climate change. *Science*, 296(5569), 895–899. <https://doi.org/10.1126/science.1069270>
- Waugh, D. W., Banerjee, A., Fyfe, J. C., & Polvani, L. M. (2020). Contrasting recent trends in Southern Hemisphere Westerlies across different ocean basins. *Geophysical Research Letters*, 47(18), e2020GL088890. <https://doi.org/10.1029/2020gl088890>
- Wills, R. C., Dong, Y., Proistosescu, C., Armour, K. C., & Battisti, D. S. (2022). Systematic climate model biases in the large-scale patterns of recent sea-surface temperature and sea-level pressure change. *Geophysical Research Letters*, 49(17), e2022GL100011. <https://doi.org/10.1029/2022gl100011>
- Wills, R. C., Schneider, T., Wallace, J. M., Battisti, D. S., & Hartmann, D. L. (2018). Disentangling global warming, multidecadal variability, and El Niño in Pacific temperatures. *Geophysical Research Letters*, 45(5), 2487–2496. <https://doi.org/10.1002/2017gl076327>
- Zhang, L., Delworth, T. L., Cooke, W., & Yang, X. (2019). Natural variability of Southern Ocean convection as a driver of observed climate trends. *Nature Climate Change*, 9(1), 59–65. <https://doi.org/10.1038/s41558-018-0350-3>